Heat Pipe Science and Technology: *An International Journal* 6(3–4) 229–239 (2015)

EVALUATION OF $CaCl_2$–SILICA GEL SORBENT FOR WATER SORPTION COOLING SYSTEMS

*Claire McCague, Khorshid Fayazmanesh, Cecilia Berlanga, & Majid Bahrami**

Laboratory for Alternative Energy Conversion (LAEC), School of Mechatronic Systems Engineering, Simon Fraser University, 250-13450 102nd Avenue, Surrey, BC, Canada, V3T 0A3

*Address all correspondence to: Majid Bahrami; E-mail: mbahrami@sfu.ca

Hygroscopic salts supported by a mesoporous matrix for improved mass transport are promising sorbents for water-based sorption cycles that operate at low pressure. In this study, loose grain composites of $CaCl_2$ supported by mesoporous silica gels with four distinct pore size distributions were prepared and compared with AQSOA FAM-Z02, a silicoaluminophosphate zeolite desiccant. A salt in silica gel sorbent consolidated with graphite flakes and binder was also analyzed. The sorbents were evaluated with a volumetric nitrogen physisorption porosimeter and thermogravimetric water vapor sorption analyzer. The hygroscopic salt filled 56–60% of the open pore volume of the mesoporous silica gel supports. Water uptake capacity of the $CaCl_2$/silica gel sorbent was up to 0.33 g per gram of dry sorbent at 12 mbar and 35°C, and sample performance was consistent through 200 wetting–drying cycles.

KEY WORDS: *calcium chloride, sorption cooling, water isotherm*

1. INTRODUCTION

The vapor compression systems commonly used for air conditioning and refrigeration consume significant amounts of electrical power and employ environmentally harmful refrigerants. The power used by HVAC systems to provide thermal comfort in residential and commercial buildings amounts to 10–20% of the total energy consumed in the developed world (Cullen and Allwood, 2010; Isaac and van Vuuren, 2009; Pérez-Lombard et al., 2008). Efficient, sustainable cooling technologies are presently the focus of significant research and development efforts. In adsorption cooling systems, evaporative cooling power is created as a porous sorbent material, which can be regenerated with thermal energy, adsorbs or absorbs a refrigerant, such as water.

Sorption cooling systems that utilize materials with low regeneration temperatures can be powered by low-grade heat sources, including solar thermal and industrial

waste heat (Wang and Oliveira, 2006).The selection of an effective sorbate–sorbent working pair for a specific adsorption system depends on the intended operating conditions, particularly the temperatures and working pressures for adsorption and desorption. Zheng et al. (2014) and Aristov (2013a) reviewed solid desiccants for sorption cooling systems and compared salt in a host matrix composites with other classes of sorbents, including silica gels, zeolites, aluminophosphates, porous polymeric metal–organic frameworks, and porous carbons. Both reviews conclude that salt in porous matrix sorbents are strong candidate materials with properties that can be tuned through selection of the host material and the salt.

The focus of this research is the preparation and evaluation of sorbent materials for water sorption systems with a target regeneration temperature of 80^{o}C, particularly $CaCl_2$–silica gel sorbents. This sorbent type was chosen for its uptake capacity and uptake rate under the desired operating conditions. Glaznev et al. (2011) compared SWS-1L, a $CaCl_2$ in SBA-15 silicate composite with microporous silica, and AQSOA FAM-Z02 silicoaluminophosphate by the large-temperature jump method and determined that it had a superior instantaneous specific cooling power. The sorbent choice is also motivated by the availability of affordable salts and silica gels, and the ease of synthesis of batches ranging from grams of material for characterization to kilograms of material for testing in a lab-scale sorption chiller.

Water-based sorption chillers operate at low pressures and sorption dynamics have proven to be very sensitive to the presence of even a fraction of a millibar of background gas, as was demonstrated by Glaznev et al. (2010) in tests of silica gel, $CaCl_2$ in silica gel, and Z02. Sorbents containing $CaCl_2$ can contribute to the corrosion of metal heat exchangers, particularly mixed metal heat exchangers susceptible to galvanic corrosion. In our lab-scale sorption chiller tests, we observed performance loss due gas released by the corrosion of a copper–aluminum sorber bed heat exchanger after a single desorption cycle and the restoration of performance with the evacuation of this background gas between cycles. However, a sorption chiller with $CaCl_2$ in mesoporous silica gel coated on an aluminum alloy heat exchanger was run for 100 cycles by Freni et al. (2007) without any trace of corrosion or performance loss.

For loose grain sorbent-heat exchanger designs, sorption kinetics studies have revealed that for grain sizes below 0.5–0.8 mm the kinetic curves do not change appreciably, for example, one layer of 0.8 mm silica gel grains can deliver the same specific cooling power as four layers of 0.2 mm grains (Sapienza et al., 2014; Aristov, 2013b; N'Tsoukpoe et al., 2014). The sorption rate depends on the transport of water vapor in the porous matrix and the dissipation of the heat of adsorption. In the case of salt in silica gel composites, absorption of water vapor by the salt dispersed in the porous matrix creates a solid hydrate, and then an aqueous solution (Ovoshchnikov et al., 2011). The solution formation complicates sorption kinetics compared to water sorbed by silica gel or zeolite surfaces.

The salt confined in the support matrix undergoes water absorption, dissolution, and dilution. The density of the solution depends on the temperature and the mass fraction of $CaCl_2$. The enthalpy of adsorption is also concentration dependent. Conde (2004) reviewed the properties of aqueous solutions of $CaCl_2$ and LiCl to generate and validate equations for the solubility boundary, vapor pressure, surface tension, dynamic viscosity, thermal conductivity, specific thermal capacity, density, and differential enthalpy of dilution.

There is a pore filling threshold where the salt solution leaks from the pores and forms a film on the surface of the silica particles. Tanashev et al. (2013) measured the change in the thermal conductivity of salt in silica composites as a function of adsorbed water and observed a steep rise when the salt solution leaked from the pores, connecting the silica gel particles and enhancing heat transfer. They found that for $CaCl_2$ and the other salts tested a steep increase of thermal conductivity occurred when the calculated volume fraction of the pores occupied with salt solution was 0.60–0.64. As salt solution leakage is detrimental to the sorption chillier performance, systems should be designed to avoid this regime of operation (Gordeeva and Aristov, 2012).

This paper presents porosimetry and water sorption measurements of $CaCl_2$ confined in silica gels with mean pore diameters ranging from 4 to 16 nm. The results are compared to the water uptake properties of commercial sorbent material AQSOA FAM-Z02.

2. EXPERIMENTAL

Chromatography-grade commercial silica gels with four distinct pore size distributions and 0.2–0.5 mm irregular-shaped grains were acquired from Silicycle, Inc. (Quebec, Canada). Concentrated salt solutions were prepared with oven dried $CaCl_2$ (Fisher Scientific). The silica gels, in 10 g to 500 g batches, were wetted with ethanol, and then an aqueous $CaCl_2$ solution was added to the silica such that complete deposition of the salt into the mesoporous silica would produce the desired product. The mixtures dried for 24 h in a fume hood, and 500 g batches were further warmed on a hot plate to accelerate drying. The damp material was baked at 200°C until judged dry by consistent successive weight measurements. The mesoporous silica, SiliaFlash types B40, B60, B90, and B150, will be referred to hereafter as S4, S6, S9, and S15, while the silica supported salt composites will be referred to as $CaCl_2$–S4, $CaCl_2$–S6, $CaCl_2$–S9, and $CaCl_2$–S15. The composites were 28 wt.% $CaCl_2$ with the exception of $CaCl_2$–S4 (30 wt.%).

Salt-in-silica-gel samples consolidated with organic binder polyvinyl pyrrolidone (PVP) (40,000 MW, Sigma Aldrich) and graphite flake (+100 mesh, <150 μm, Sigma Aldrich) as a thermally conductive additive were prepared in small batches. The components were combined in an aqueous solution that was dried on a hot plate, and then heated to 180°C to cross-link the polymer. The product, $CaCl_2$–S15G, was 30% $CaCl_2$, 30% silica, 15% PVP, and 25% graphite flake by weight. Sili-

coaluminophosphate desiccant AQSOA FAM-Z02 was acquired from Mitsubishi Plastics. This zeolite, referred to hereafter as Z02, was in the form of 1.8–2 mm diameter pellets containing 6–17 wt.% silicon dioxide binder.

Nitrogen isotherms at 77 K were collected with a volumetric gas adsorption analyzer (ASAP 2020, Micromeritics Instrument Corp., USA) to determine the textural characteristics of the silica gels and composites. The samples were degassed under vacuum at 150°C for one hour, followed by two hours at 200°C prior to the measurements. The Brunauer, Emmett, and Teller (BET) model was used to calculate the specific surface area, S_{BET} (Brunauer et al., 1938). Incremental pore volume per pore width distributions were calculated from the adsorption branch of the isotherm using the Barrett, Joyner, and Halenda (BJH) model (Barrett et al., 1951).

Water sorption isotherms were collected with a thermogravimetric analyzer (TGA) (IGA-002, Hiden Isochema, UK). The samples were dried under vacuum at 200°C for six hours to determine their dry weight. Multiple isotherms were collected for each sample without repeating the drying process. That is, each isotherm ended with a final desorption, outgassing step at the isotherm temperature, and the next isotherm began after the automated system adjusted the sample temperature. The kinetic data for each pressure step were analyzed by a real time processor, and successive pressure steps were taken when water sorption was 98.5% of the predicted equilibrium. The water uptake was calculated either as

$$w\,(g_{H_2O}/g_{sorbent}) = m/m_{dry}$$

or

$$N\,(\text{mole}_{H_2O}/\text{mole}_{CaCl_2}) = \frac{m/M_{H_2O}}{(m_{dry}\,C)/M_{CaCl_2}},$$

where the molar masses, M, of H_2O and $CaCl_2$ are 18.15 g/mol and 110.98 g/mol, respectively, and C is the wt.% of salt in the composite. Short-term durability studies of the $CaCl_2$–S15 composite were conducted with the TGA through 200 pressure swing cycles at 35°C, whereby the sample was exposed to alternating 12 mbar H_2O and vacuum outgassing conditions.

3. RESULTS

The N_2 adsorption/desorption isotherms of the silica gels and $CaCl_2$/silica composites were Type IV with H1 hysteresis loops, typical of mesoporous materials. The isotherms for the $CaCl_2$–S4 and $CaCl_2$–S15 composites and their pure silica gel supports are shown in Fig. 1, and the calculated textural characteristics are summarized in Table 1. Consistent with previous reports, the results indicate that $CaCl_2$ fills the silica gel pores and decreases the specific surface area and pore volume. The high uncertainty in pore size distributions calculated from the adsorption

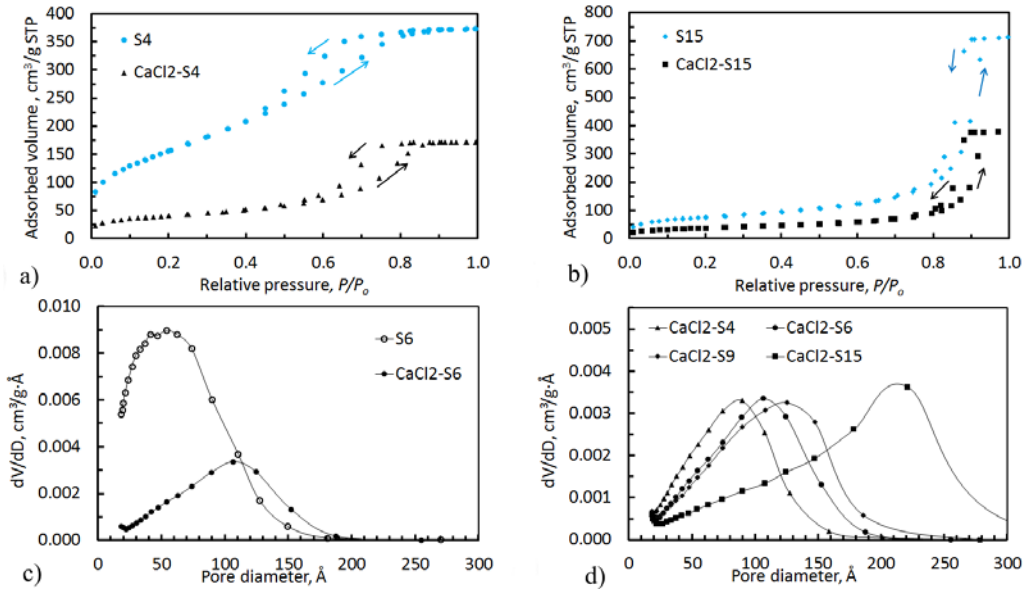

FIG. 1: Comparison of the N_2 isotherms for: a) S4 and $CaCl_2$–S4, b) S15 and $CaCl_2$–S15; comparison of qualitative incremental pore volume per pore width for: c) S4 and $CaCl_2$–S4 and d) $CaCl_2$ supported by different silica gels

branch of N_2 isotherms by the BJH method has been recently discussed by De Lange et al. (2014). The incremental pore volume per pore width curves in Fig. 1 provide a qualitative indication of the change in the pore size distribution of $CaCl_2$–B6 relative to B6, specifically the decrease in pore volume and change in the pore size distribution due to the preferential filling of small pores. The qualitative relative differences in the pore sizes distributions of the different silica gel salt composites prepared for this study are also shown. $CaCl_2$–S4 and $CaCl_2$–S15, the samples with the greatest difference in pore size distribution, were selected for detailed comparison of their water sorption characteristics.

TABLE 1: Textural characteristics of samples calculated from N_2 adsorption isotherms

No.	S_{BET}, $m^2 \cdot g^{-1}$	Pore volume, $cm3 \cdot g^{-1}$	Mean pore diameter, nm	No.	S_{BET}, $m^2 \cdot g^{-1}$	Pore volume, $cm^3 \cdot g^{-1}$	Mean pore diameter, nm
S4	574 ± 2	0.58	4	$CaCl_2$–S4	146.7 ± 0.5	0.27	7
S6	487 ± 2	0.75	6	$CaCl_2$–S6	134.5 ± 0.4	0.37	9
S9	406 ± 0.4	0.83	8	$CaCl_2$–S9	148.3 ± 0.4	0.58	10
S15	276 ± 0.8	1.10	16	$CaCl_2$–S15	136.3 ± 0.4	0.60	18

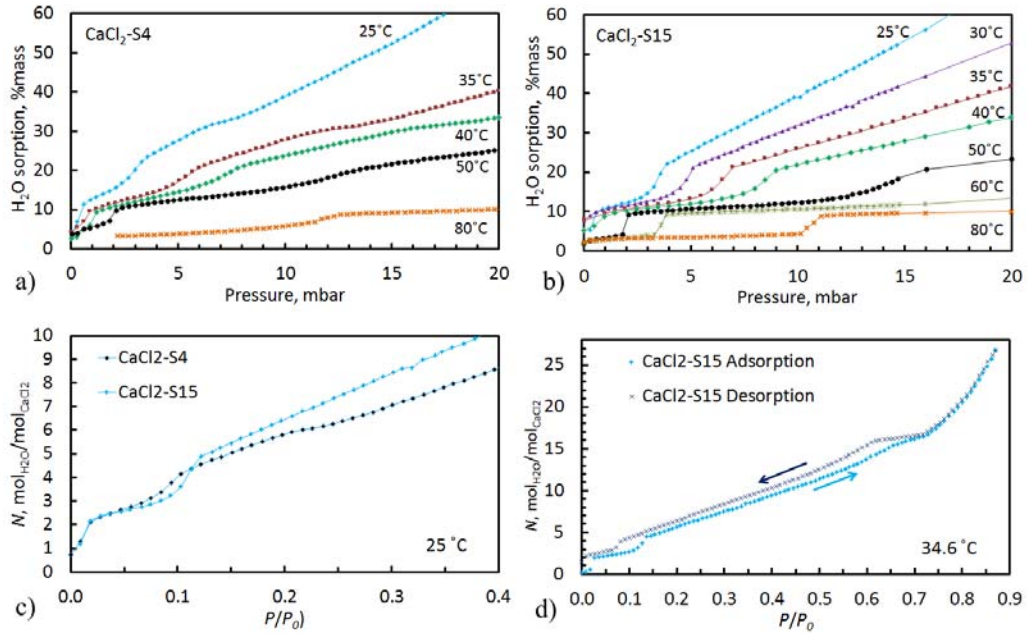

FIG. 2: Water sorption isotherms from 25 to 80°C for: a) $CaCl_2$–S4, b) $CaCl_2$–S15; water sorption isotherms of: c) $CaCl_2$ in S4 and S15 in mole H_2O per mole $CaCl_2$ at 25°C; d) $CaCl_2$–S15 to high partial pressure at 35°C

The water adsorption branch of the complex isotherms of $CaCl_2$–S4 and $CaCl_2$–S15 collected at temperatures from 25 to 80°C are shown in Fig. 2. The initial transition from $CaCl_2$ to $CaCl_2{\cdot}2H_2O$ (~10 wt.%) is most clearly shown in the 50°C and 80°C curves, occurring near 2 mbar and 11 mbar, respectively. The transition is steeper for $CaCl_2$–S15 compared to $CaCl_2$–S4, as is the next increase in curvature occurring at ~12 mbar on both of the 50°C curves. This distinctive difference between the adsorption of $CaCl_2$ in S4 versus S15 is seen more completely in the 35°C curves, as a bulge on the $CaCl_2$–S4 isotherm from 4–14 mbar. The equivalent features are subtler in the $CaCl_2$–S15 isotherm, but the end of this region is visible as a single point divot at 10.1 and 12.6 mbar in the 25°C and 35°C curves, respectively. This difference is further illustrated by the plots of N (mole H_2O per mole $CaCl_2$) as a function of relative pressure, P/P_0, for $CaCl_2$–S4 and $CaCl_2$–S15 at 25°C as shown in Fig. 2c. When plotted as a function of relative pressure, P/P_0, the isotherms collected at different temperatures were parallel with slightly lower sorption capacity with increasing temperature. The offset reflects the strong $CaCl_2$–water interactions, however, we have not yet ruled out the possibility of a contribution from instrumental systematic error, such as an imperfect buoyancy correction.The complex shape of the sorption–desorption isotherm to ~$0.9P/P_0$ at 35°C for $CaCl_2$–S15 is shown in Fig. 2d.

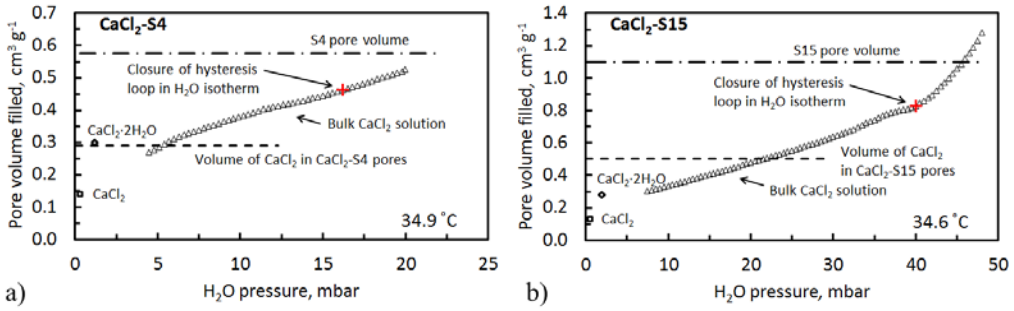

FIG. 3: Comparison of measured pore volume for: a) S4 and $CaCl_2$–S4, b) S15 and $CaCl_2$–S15 from N_2 isotherms with H_2O isotherm "pores filled" point (+), and calculated volume of $CaCl_2$ (□), $CaCl_2$–$2H_2O$ (◇), and $CaCl_2$ solution (Δ) calculated from the mass of sorbed water as a function of pressure and associated $CaCl_2$ molar fraction

As the salt absorbs water, it transforms into solid $CaCl_2{\cdot}2H_2O$, and then deliquesces. The bulk melting point of $CaCl_2{\cdot}4H_2O$ is 45°C (Molenda et al., 2013, however the melting point of salt confined in silica is known to be depressed. Following the equations of Conde (2004), the density of aqueous $CaCl_2$ solutions can be calculated as a function of the mole fraction of the salt relative to the water. In Fig. 3, the weight of water adsorbed as a function of pressure and the weight of salt in the composite are used to estimate the volume of solution in the composite at various vapor pressures. However, the capillary forces between the solution and porous matrix are known to affect the solution density. On each curve, the vapor pressure at which the upper closure of the hysteresis loop occurs in the water sorption isotherms is marked. At this point, the pores are filled with solution, and the change of curvature of the isotherm above this point reflects the transition to sorption into the salt solution that has leaked into the interparticle space between the silica gel grains (Fig. 2d). The upper closure point of the hysteresis loops for $CaCl_2$–S4 and $CaCl_2$–S15 occurred at 16 mbar and 40 mbar H_2O, respectively, when the calculated volume fraction filled was only 0.8 and 0.74.

The upper dashed lines in the plots in Fig. 3 show the pore volume of silica gel host matrices, S4 and S15, and the lower dashed lines indicate the measured fraction of that pore volume filled by $CaCl_2$ in the salt–silica composites. Both these values were determined by nitrogen porosimetry. It is shown that the volume filled by salt far exceeds the volume calculated from the weight of $CaCl_2$ and its bulk density, 2.15 $g{\cdot}cm^{-3}$. The measured volume filled by dry $CaCl_2$ suggests that the density of the deposited $CaCl_2$ is low, even comparable to the density of concentrated aqueous $CaCl_2$ solutions. Alternatively, $CaCl_2$ could be blocking but not filling some of the pores, resulting in the lower pore volume of the composite.

The water sorption, pressure, and temperature for 12 mbar pressure swing tests of $CaCl_2$–S15G and Z02 are shown in Fig. 4. During tests, a water bath at 35°C

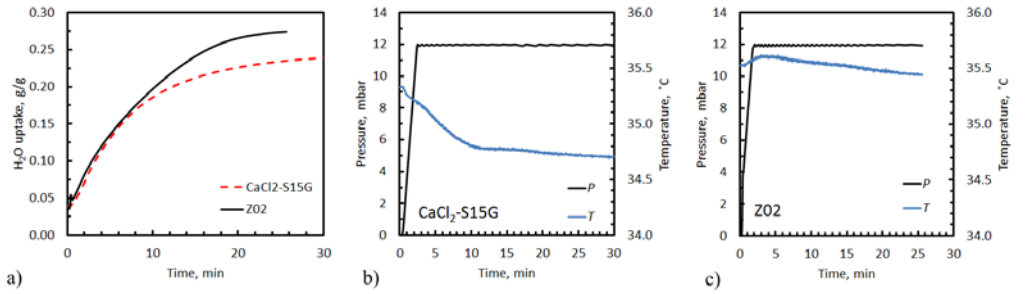

FIG. 4: a) Water sorption as a function of time for a 12 mbar pressure swing for Z02 and $CaCl_2$–S15G (g/g total weight of composite). Test pressure and temperature conditions for; b) $CaCl_2$–S15G; c) Z02

surrounds the reactor cylinder and the temperature readings are from a thermometer directly adjacent to the sample. From these curves, near equivalent specific cooling powers for cycles to 80% of the sorption capacity, $\Delta w_{0.8}$, were calculated as $W_{0.8} = \Delta w_{0.8}\,\Delta H_{vap}\,/\tau_{0.8}$, where $\tau_{0.8}$ is the uptake time and ΔH_{vap} is the heat of vaporization of water, 2478 kJ/kg. Under these test conditions, the specific cooling power of $CaCl_2$–S15G, containing 25 wt.% graphite flakes and 15 wt.% binder, was 0.54 kW/kg compared to 0.60 kW/kg for the benchmark material, Z02, as summarized in Table 2. The sorption performance of $CaCl_2$–S15 was tested for 200, 20 min pressure swing cycles at 35°C and found to be consistent with and initial and final Δw_{cycle} of 0.196 and 0.195 g/g. Review of the detailed data indicated that both the adsorption step final weight and desorption step final weight increased slightly during the 200 cycle run, the difference in these increases created the 0.001 drop in Δw_{cycle}. The water sorption isobars for $CaCl_2$–S15 and Z02 are presented in Fig. 5 along with the equilibrium adsorption times for 0–12 mbar pressure swings at each temperature. It is of note that the uptake rate for Z02 declines significantly at ~40°C, ahead of the temperature where there is a sharp drop in the uptake capacity.

The water sorption isosters for $CaCl_2$–S15 and Z02 are plotted in the ln (P_{H_2O}) versus $1/T$ form in Fig. 6 for various amounts of sorbed water, w (g/g).

The isosteric heat of water sorption is determined as a function of the slope of the linear isosters, where $\ln(P) = B(w)/T + C(w)$ and $\Delta H_{is}(w) = B(w)\,R$ and R is

TABLE 2: Uptake, time, and power for pressure swing cycles (0–12 mbar) for 80% equilibrium sorption capacity

Sample	T, °C	Dry wt., mg	$w_{initial}$, g/g	w_{final}, g/g	$\Delta w_{0.8}$, g/g	$\tau_{0.8}$, min	$W_{0.8}$, kW/kg
$CaCl_2$–S15G	35	21.231	0.038	0.241	0.163	13.0	0.54
Z02	35	19.358	0.036	0.274	0.190	12.5	0.60

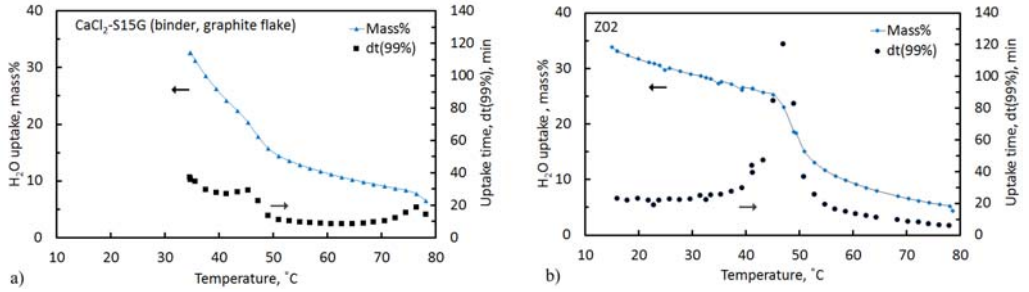

FIG. 5: Water sorption isobars at 12 mbar and the equilibrium adsorption time (dt 99%) for 0–12 mbar pressure swings at each temperature for a) $CaCl_2$–S15G (mass % based on the dry weight of sorbing ingredients, $CaCl_2$, S15, and binder with the graphite flake weight excluded) and for b) ASQOA FAM-Z02 pellets

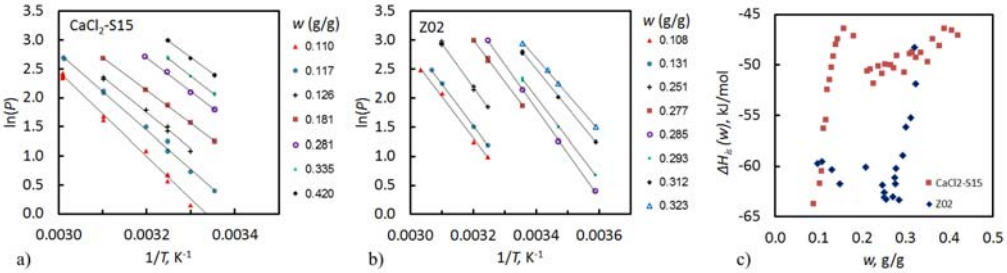

FIG. 6: Isosters for a) $CaCl_2$–S15 and b) Z02; c) isosteric water sorption heat for $CaCl_2$–S15 and Z02

the universal gas constant. The increase in $\Delta H_{is}(w)$ to –63.7 kJ/mol as w approaches 0.09 (N = 2) is due to the formation of solid hydrates with more strongly bound water molecules, and is consistent with reports from Aristov et al. (1996) (62.3 kJ/mol isosteric desorption) for $CaCl_2$ in mesoporous silica gel.

4. CONCLUSIONS

Water sorbent composites of $CaCl_2$ supported by mesoporous silica gels were prepared and characterized. The water isotherms of $CaCl_2$ in silica gels with 4 nm and 16 nm average pore sizes were compared. The pore volume filled by solid $CaCl_2$ and concentrated aqueous $CaCl_2$ was measured and calculated for use in future diffusivity calculations through analysis small pressure step isotherms. Water uptake capacity of the $CaCl_2$/silica gel sorbent was up to 0.33 g per gram of dry sorbent at 12 mbar and 35°C, and sample performance was consistent through 200 wetting–drying cycles. The isobars, isosters, and isosteric enthalpy of water sorption of $CaCl_2$–S15 and silicoaluminophosphate desiccant, Z02 were measured and compared.

ACKNOWLEDGMENTS

The authors gratefully acknowledge the financial support of the Natural Sciences and Engineering Research Council of Canada (NSERC) through Automotive Partnership Canada Grant No. APCPJ 401826-10. We thank Dr. D. Leznoff and Ryan Roberts for their assistance with nitrogen adsorption experiments.

REFERENCES

Aristov, Y., Challenging offers of material science for adsorption heat transformation: A review, *Appl. Therm. Eng*., vol. **50**, pp. 1610–1618, 2013a.

Aristov, Y., Experimental and numerical study of adsorptive chiller dynamics: Loose grains configuration, *Appl. Therm. Eng*., vol. **61**, pp. 841–847, 2013b.

Aristov, Y., Tokarev, M., Cacciola, G., and Restuccia, G., Selective water sorbents for multiple applications. 1. CaCl2 confined in mesopores of silca gel: sorption properties, *React. Kinet. Catal. Lett*., vol. **59**, pp. 325–333, 1996.

Barrett, E., Joyner, L., and Halenda, P., The determination of pore volume and area distributions in porous substances, computations from nitrogen isotherms, *J. Am. Chem. Soc*., vol. **73**, pp. 373–380, 1951.

Brunauer, S., Emmett, P., and Teller, E., Adsorption of gases in multimolecular layers, *J. Am. Chem. Soc*., pp. 309–319, 1938.

Conde, M., Properties of aqueous solutions of lithium and calcium chlorides: formulations for use in air conditioning equipment design, *Int. J. Therm. Sci*., vol. **43**, pp. 367–382, 2004.

Cullen, J. and Allwood, J., The efficient use of energy: Tracing the global flow of energy from fuel to service, *Energy Policy*, vol. **38**, pp. 75–81, 2010.

De Lange, M., Vlugt, T., Gascon, J., and Kapteijin, F., Adsorptive characterization of porous solids: Error analysis guides the way, *Micropor. Mesopor. Mat.*, vol. **200**, pp. 199–215, 2014.

Freni, A., Russo, F., Vasta, S., Tokarev, M., Aristov, Y. I., and Restuccia, G., An advanced solid sorption chiller using SWS-1L, *Appl. Therm. Eng.*, vol. **27**, pp. 2200–2204, 2007.

Glaznev, I., Ovoshchnikov, D., and Aristov, Y. I., Effect of residual gas on water adsorption dynamics under typical conditions of an adsorption chiller, *Heat Transf. Eng*., vol. **31**, pp. 924–930, 2010.

Glaznev, I., Ponomarenko, I., Kirik, S., and Aristov, Y. I., Composites $CaCl_2$/SBA-15 for adsorptive transformation of low temperature heat: Pore size effect, *Int. J. Refrig*., vol. **34**, pp. 1244–1250, 2011.

Gordeeva, L. and Aristov, Y. I., Composites 'salt inside porous matrix' for adsorption heat transformation: a current state-of-the-art and new trends, *Int. J. Low-Carbon Tech*., vol. **7**, pp. 288–302, 2012.

Isaac, M. and van Vuuren, D., Modeling global residential sector energy demand for heating and air conditioning in the context of climate change, *Energy Policy*, vol. **92**, pp. 507–521, 2009.

Molenda, M., Stengler, J., Linder, M., and Worner, A., Reversible hydration behavior of $CaCl_2$ at high H_2O partial pressures for thermochemical energy storage, *Thermochimica Acta*, vol. **560**, pp. 76–81, 2013.

N'Tsoukpoe, K., Restuccia, G., Schmidt, T., and Py, X., The size of sorbents in low pressure sorption or thermochemical energy storage processes, *Energy*, vol. **77**, pp. 983–998, 2014.

Ovoshchnikov, D., Glaznev, I., and Aristov, Y. I., Water sorption by the calcium chloride/silica gel composite: The accelerating effect of the salt solution present in the pores, *Kinet. Catal*., vol. **52**, pp. 620–628, 2011.

Perez-Lombard, L., Ortiz, J., and Pout, C., A review on buildings energy consumption information, *Energ Buildings*, vol. **40**, pp. 394–398, 2008.

Sapienza, A., Santamaria, S., Frazzica, A., Freni, A., and Aristov, Y. I., Dynamic study of adsorbers by a new gravimetric version of the large temperature jump method, *Appl. Energy*, vol. **113**, pp. 1244–1251, 2014.

Tanashev, Y., Krainov, A., and Aristov, Y. I., Thermal conductivity of composite sorbents "salt in porous matrix" for heat storage and transformation, *Appl. Therm. Eng*., vol. **61**, pp. 401–407, 2013.

Wang, R. and Oliveira, R., Adsorption refrigeration — An efficient way to make good use of waste heat and solar energy, *Prog. Energ. Combust. Sci*., vol. **32**, pp. 424–458, 2006.

Zheng, X., Ge, T., and Wang, R., Recent progress on desiccant materials for solid desiccant cooling, *Energy*, vol. **74**, pp. 280–294, 2014.